

Predicting Unsteady Flow Parameters in a Subsonic Air Diffuser Using MacCormack's Explicit Method

Tawfeeq Wasmi M. Salih

Al-Mustansiriyah University, Materials Engineering Department

**Corresponding author tawfeeqwasmi@uomustansiriyah.edu.iq

Submitted: 17/5/2017

Accepted: 8/8/2018

Abstract: A numerical procedure is presented to predict the flow characteristics inside a subsonic diffuser by solving Navier-Stokes' equations, using MacCormack's explicit method. The flow is assumed to be viscous, compressible, unsteady and two-dimensional. The grid model suggested for the diffuser has 20 points in the horizontal direction and 30 points in the vertical direction. The numerical solution has shown reasonable results with a 2D variation of flow properties inside the diffuser and the steady state solution can be satisfied by 600-900 loops only. The obtained results of the present study are compared with those obtained by using a numerical code of National Project for Application-oriented Research in CFD (NPARC) as well as those obtained from a previous experimental study and give an acceptable range of errors (about $\pm 15\%$).

Keywords: Subsonic flow, Navier-Stokes equations, CFD, Fluid mechanics, Gas-dynamics

توقع متغيرات التدفق غير المستقر في ناشر الهواء دون سرعة الصوت باستخدام طريقة

ماكورماك الصريحة

توفيق وسمي محمد صالح

الخلاصة: تم في هذا البحث تقديم طريقة عددية لتوقع متغيرات التدفق داخل ناشر هواء دون سرعة الصوت عن طريق حل معادلات نافير-ستوكس باستخدام طريقة ماكورماك الصريحة. ويفترض الحل تدفق لزج طباقى مضغوط غير مستقر وثلاثي الأبعاد. يتكون نموذج الشبكة المقترح للناشر من 20 نقطة في الاتجاه الأفقي و 30 نقطة في الاتجاه الرأسي. لقد أظهر الحل العددي نتائج مقبولة لقيم متغيرات الجريان (السرعة والضغط والكثافة ودرجة الحرارة) حيث تبين أن عدد التكرارات المطلوبة للوصول إلى حالة الاستقرار يمكن أن تكون (600-900) فقط. تمت مقارنة النتائج التي تم الحصول عليها من هذه الدراسة مع دراسة عددية معتمدة على الكود (NPARC) وكذلك دراسة تجريبية سابقة مقارنة وأعطت مديات مقبولة من الأخطاء بحدود ($\pm 15\%$).

1. INTRODUCTION

The main goal of the diffuser is to reduce the flow velocity and also to recover the static pressure of the flow. The applications of diffusers can be mostly witnessed in gas turbines, combustion chambers and in aerodynamics. The effect of compressibility on flow is absolutely necessary for these applications. The Navier-Stokes equations are dominant in the viscous regions, but the majority of air flow situations encountered in the industry and nature have high Reynolds numbers, thus they have been considered as inviscid flows and have reduced the equation to Euler equations [1]. However, compressible flows, with moderate Reynolds numbers, in channels of variable cross-sections also frequently use the Navier-Stokes in several branches of contemporary technology such as in spray processes, production of micro metallic particles, and design of valveless pumps [2]. In the case of a continuous subsonic flow, the calculation of flow parameters inside a diffuser flow can be accomplished by solving the Navier-Stokes's equations for the entire flow field, where the pressure change is very small. On the other hand, variations in velocity and pressure appear because of changes in density, due to the compressible flow field. As a result, the flow parameters are consequently solved through the solving of: mass, linear momentum, energy and an equation of state [3].

Usually, any numerical simulation aims to perform a smooth, easy, and precise procedure for certain domains by employing suitable initial conditions and boundary conditions [4]. The enhancement of numerical simulation of fluids and heat transfer problems needs to satisfy a convergence technique according to advanced grid generation as well as high speed computers. In recent times, many schemes have been developed to solve Euler equations and Navier-Stokes equations for different applications [5]. However, the numerical solutions of subsonic air flow in conduits and channels exhibit greater regularity than that of a supersonic flow.

The turbulent air flow in a conical subsonic diffuser was studied by Dudek et al [6], using a numerical code of (NPARC). The geometry of the diffuser is assumed to be axisymmetric, with 0.154 m at the entrance and inclined

by 5°, up to a length of 0.642 m. The core flow velocity at the entrance was assumed to be 52 m/s. The grid had 120 x 70 points and the number of iterations required to satisfy the steady-state solution was 60000. The results presented the velocity profile and the pressure gradient along the diffuser. Abbood [7] has introduced a solution for choked flow in a convergent-divergent nozzle based on MacCormack's scheme, where the behavior of velocity and pressure was very useful. The flow was assumed to be unsteady, compressible and inviscid. The grid generation technique that was used for the nozzle had 20 x 20 points. Steady state solution was obtained in about 1000 iterations. A research by Rosello [8] has presented a new numerical approach to solve the Euler equations for low Mach number flows based on the Cauchy-Kovalevskaya theorem and Frobenius algorithm. The study claimed that the technique used had reasonable and satisfactory results in contrast to the MacCormack scheme, and it was advised to use a Courant-Friedrichs-Lewy (CFL) factor of 0.01, which was successfully used for these kinds of problems.

Jalal and Ahmed [9] have studied the two-dimensional ramp inlet flow fields using Euler equations. A solution algorithm based on the finite difference in the MacCormack's technique was developed to solve mixed subsonic-supersonic flow regions, through shocks. It is observed that a value of 0.1 CFL factor is successful to solve the problem. Sinha et al [10] have investigated the performance characteristics in an annular subsonic diffuser using the numerical code FLUENT. The results have validated the experimental data obtained by using a series of parametric investigations. The velocity profiles indicate fluid accumulation at the wall of the exit section due to the combined effect of velocity diffusion and centrifugal action. The maximum value of the static pressure recovery is 27% compared to the predicted results of 31%, thus closed to that obtained experimentally. A numerical and experimental study of an intake lip shaping was conducted by Berens [11], to improve assessment of the sources of the aerodynamic forces. The impact of the boundary layer on the total pressure recoveries was investigated as well. The internal flow was studied numerically by employing the EIKON configuration model for the complicated Navier-Stokes computations in the simulated intake duct. Numerical results show convergent values with the experimental data obtained for the total pressure recovery. Some discrepancies are found between numerical results and experimental data and that is mainly due to the lack of accuracy and divergence in some regions.

The present study investigates the flow parameters (velocity, pressure, temperature, and density) in a subsonic diffuser for certain assumptions and conditions that are not mentioned by other numerical studies as a total package, where the MacCormack explicit scheme has been used with modified steps. The flow is assumed as unsteady, compressible, viscous (laminar), and two-dimensional. The suggested geometry for the present study is shown in Figure 1, where only half of the diffuser can be considered in the calculations due to its axisymmetric shape. This geometry is suggested in order to simulate the dimensions that are mentioned by Dudek et al [6], for the purpose of comparison only.

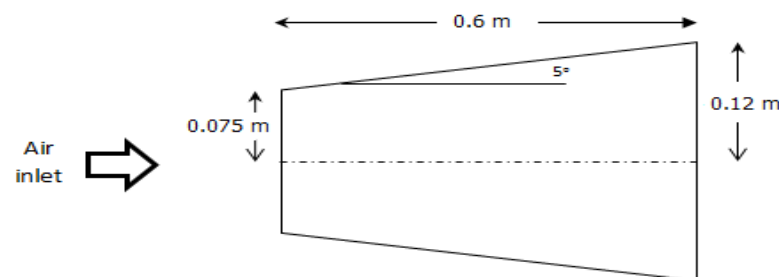


Figure 1 Geometry of the diffuser

2. MATHEMATICAL MODEL

The aim of the numerical procedure is to solve the Navier-Stokes equations for the assumptions proposed in a linear subsonic diffuser using the MacCormack's explicit method, which is much easier and can approach the steady-state conditions faster. In fluid dynamics, Navier-Stokes are a set of quasi-linear hyperbolic equations that represent: the conservation of mass (continuity), balance of forces (momentum), and balance of energy. The governing equations of the two-dimensional flow for the mentioned assumptions are found in Anderson et al [12]:

Continuity:

$$\frac{\partial \rho}{\partial t} + \frac{\partial(\rho u)}{\partial x} + \frac{\partial(\rho v)}{\partial y} = 0 \quad (1)$$

X-momentum:

$$\frac{\partial(\rho u)}{\partial t} + \frac{\partial(\rho u^2)}{\partial x} + \frac{\partial(\rho uv)}{\partial y} + \frac{\partial P}{\partial x} = \mu \left(\frac{\partial^2 u}{\partial x^2} + \frac{\partial^2 u}{\partial y^2} \right) \quad (2)$$

Y-momentum:

$$\frac{\partial(\rho v)}{\partial t} + \frac{\partial(\rho uv)}{\partial x} + \frac{\partial(\rho v^2)}{\partial y} + \frac{\partial P}{\partial y} = \mu \left(\frac{\partial^2 v}{\partial x^2} + \frac{\partial^2 v}{\partial y^2} \right) \quad (3)$$

Energy:

$$\frac{\partial E_t}{\partial t} + \frac{\partial(E_t + P)u}{\partial x} + \frac{\partial(E_t + P)v}{\partial y} = 0 \quad (4)$$

where:

$$E_t = \rho \left(e + \frac{V^2}{2} \right) \quad (5)$$

$$V^2 = u^2 + v^2 \quad (6)$$

After rearrangement, the governing equations can be written as:

Continuity:

$$\frac{\partial \rho}{\partial t} = - \left[\rho \frac{\partial u}{\partial x} + u \frac{\partial \rho}{\partial x} + \rho \frac{\partial v}{\partial y} + v \frac{\partial \rho}{\partial y} \right] \quad (7)$$

X-momentum:

$$\frac{\partial u}{\partial t} = - \left[u \frac{\partial u}{\partial x} + v \frac{\partial u}{\partial y} + \frac{1}{\rho} \frac{\partial P}{\partial x} \right] + \frac{\mu}{\rho} \left(\frac{\partial^2 u}{\partial x^2} + \frac{\partial^2 u}{\partial y^2} \right) \quad (8)$$

Y-momentum:

$$\frac{\partial v}{\partial t} = - \left[u \frac{\partial v}{\partial x} + v \frac{\partial v}{\partial y} + \frac{1}{\rho} \frac{\partial P}{\partial y} \right] + \frac{\mu}{\rho} \left(\frac{\partial^2 v}{\partial x^2} + \frac{\partial^2 v}{\partial y^2} \right) \quad (9)$$

Energy:

$$\frac{\partial e}{\partial t} = \left[u \frac{\partial e}{\partial x} + v \frac{\partial e}{\partial y} + \frac{P}{\rho} \frac{\partial u}{\partial x} + \frac{P}{\rho} \frac{\partial v}{\partial y} \right] \quad (10)$$

3. NUMERICAL SOLUTION

The numerical solution starts after converting the governing equations from a partial differential (PD) form to a finite difference (FD) form in order to apply the MacCormack's explicit method, which includes the predictor step as well as the corrector step. In any numerical solution, three important elements are required: Mesh generation, initial conditions, and boundary conditions. Figure 2 shows the procedure followed by the current study.

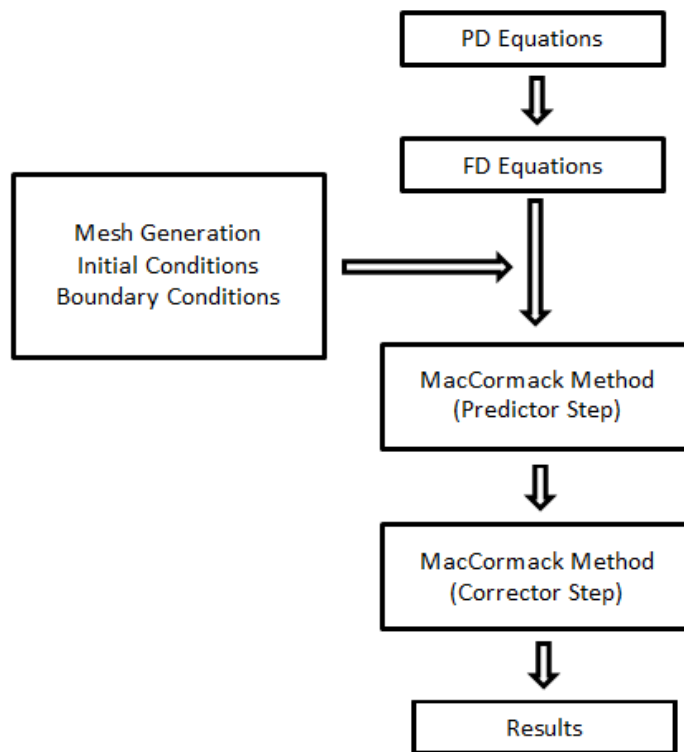


Figure 2 Procedure followed by the current study

3.1 MacCormack's Explicit Method

This scheme is second-order accurate in both space and time. It consists of two steps: Predictor and corrector. The forward finite difference method (FFDM) is used for all spatial derivatives in the predictor step, even as the backward finite difference method (BFDM) is used in the corrector step.

The governing continuity equation in forward form (FFDM) is written as:

$$\left(\frac{\partial \rho}{\partial t}\right)_p = - \left[\rho_{i,j} \frac{u_{i+1,j} - u_{i,j}}{\Delta x} + u_{i,j} \frac{\rho_{i+1,j} - \rho_{i,j}}{\Delta x} + \rho_{i,j} \frac{v_{i,j+1} - v_{i,j}}{\Delta y} + v_{i,j} \frac{\rho_{i,j+1} - \rho_{i,j}}{\Delta y} \right] \quad (11)$$

This is called the predictor step, and then the corresponding properties can be calculated as:

$$\rho_{i,j_c} = \rho_{i,j} + \left(\frac{\partial \rho}{\partial t}\right)_p \Delta t \quad (12)$$

The governing continuity equation in backward form (BFDM) is written as:

$$\left(\frac{\partial \rho}{\partial t}\right)_c = - \left[\rho_{i,j_c} \frac{u_{i,j_c} - u_{i-1,j_c}}{\Delta x} + u_{i,j_c} \frac{\rho_{i,j_c} - \rho_{i-1,j_c}}{\Delta x} + \rho_{i,j_c} \frac{v_{i,j_c} - v_{i,j-1_c}}{\Delta y} + v_{i,j_c} \frac{\rho_{i,j_c} - \rho_{i,j-1_c}}{\Delta y} \right] \quad (13)$$

This is called the corrector step, and then the new values of the properties (next time) can be calculated as:

$$\rho_{i,j_n} = \rho_{i,j} + \left(\frac{\partial \rho}{\partial t}\right)_M \Delta t \quad (14)$$

Where:

$$\left(\frac{\partial \rho}{\partial t}\right)_M = 0.5 \left[\left(\frac{\partial \rho}{\partial t}\right)_p + \left(\frac{\partial \rho}{\partial t}\right)_c \right] \quad (15)$$

By the same procedure, we can adapt other conservations equations (momentum and energy) to obtain:

$$u_{i,j_n} = u_{i,j} + \left(\frac{\partial u}{\partial t} \right)_M \Delta t \quad (16)$$

$$v_{i,j_n} = v_{i,j} + \left(\frac{\partial v}{\partial t} \right)_M \Delta t \quad (17)$$

$$e_{i,j_n} = e_{i,j} + \left(\frac{\partial e}{\partial t} \right)_M \Delta t \quad (18)$$

On account of the complexity of these equations, it is required to follow an empirical formula for each grid point before the computation and then use the smallest value for the solution [12].

$$\Delta t \leq \frac{\sigma CFL}{1 + \frac{2}{Re}} \quad (19)$$

Where;

$$Re = \frac{\rho u \Delta x}{\mu} \quad (20)$$

Also, σ is the safety factor (0.85); while, Δx and Δy are the grid steps in the horizontal and vertical directions, respectively.

The Courant-Friedriches-Lowry (CFL) factor is calculated from [12]:

$$CFL = \left[\frac{|u|}{\Delta x} + \frac{|v|}{\Delta y} + a \sqrt{\left(\frac{1}{\Delta x} \right)^2 + \left(\frac{1}{\Delta y} \right)^2} \right]^{-1} \quad (21)$$

Where;

$$a = \sqrt{\gamma RT} \quad (22)$$

It is also advised to use the perfect gas equation in order to satisfy the requirements of the solution for whole unknowns. Hence;

$$P = \rho RT \quad (23)$$

3.2 Mesh Generation

Grid generation is a procedure usually applied to get: Accurate, relaxed, and fast numerical solutions. This technique includes many steps like: grid orientation, discretization, computations, and finally achieving a convergence with strategies, to minimize the operational iterations. The grid used for the axisymmetric diffuser is assumed to be 20 horizontal points versus 30 vertical points, as shown in Figure 3.

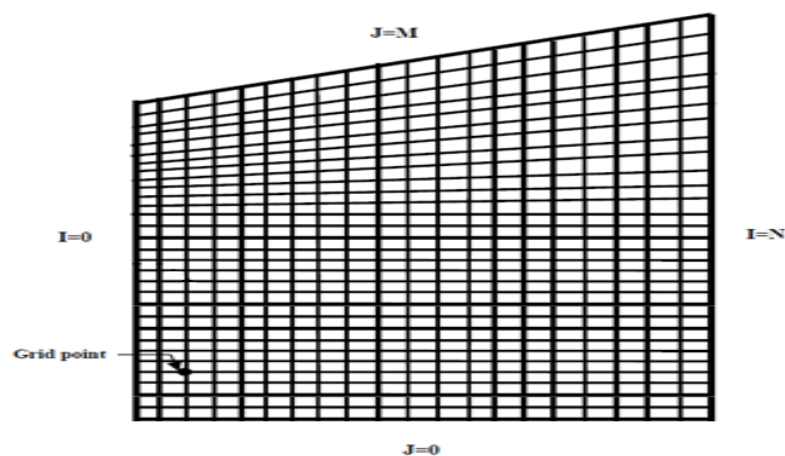


Figure 3 Entire meshes over the diffuser including 20 x 30 points

3.3 Initial Conditions

The governing equations are presented in one-dimensional form and are solved to obtain the results that would be the best initial conditions that satisfy less iteration to approach the steady state solution. The obtained results could be generalized for the two-dimensional grid points, where initial values are considered constant for a certain column. The continuity, momentum, energy, and equation of state could be presented in 1-dim form as follows [13]:

Continuity

$$\frac{d\rho}{\rho} + \frac{dA}{A} + \frac{dV}{V} = 0 \quad (24)$$

Momentum:

$$P A + \left(P + \frac{dP}{2} \right) dA - (P + dP) (A + dA) = \rho A V dV \quad (25)$$

Energy

$$dq = C_p dT \quad (26)$$

Equation of state

$$\frac{dP}{P} = \frac{d\rho}{\rho} + \frac{dT}{T} \quad (27)$$

After deriving and rearrangement, it leads to:

$$dP = \rho V^2 \frac{\left(\frac{dA}{A} - \frac{dq}{C_p T} \right)}{1 - \frac{\rho V^2}{P}} \quad (28)$$

Thus,

$$P_2 = P_1 + dP \quad (29)$$

Where, (1) refers to inlet flow from an element
(2) refers to outlet flow from an element

The other properties are calculated from:

$$T_2 = T_1 + \frac{dq}{C_p} \quad (30)$$

$$\rho_2 = \frac{P_2}{R T_2} \quad (31)$$

$$V_2 = \frac{\dot{m}}{\rho_2 A_2} \quad (32)$$

Where the cross sectional area (A) and the mass flow rate (\dot{m}) is calculated by:

$$A_2 = A_1 + dA \quad (33)$$

$$\dot{m} = \rho v A \quad (34)$$

3.4 Boundary Conditions

A set of boundary conditions must be specified analytically and then it should be transferred into a numerical formula. For the problem under consideration, there are four types of boundaries: Centerline, solid wall, inflow, and outflow. Normally, there are two kinds of conditions at the wall, either the value at boundary is given, or the value component normal to the boundary is specified (slip condition). For the present study, the suitable boundary conditions are:

$$I=0 \quad \text{Constant properties at diffuser inlet } \& v=0$$

$$J=0 \quad P = P_{One-Dim}, u = U_{One-Dim}, v=0$$

$$J=30 \quad \frac{\partial P}{\partial y} = 0, u = 0, v = 0$$

$$I=20 \quad \frac{\partial P}{\partial x} = 0, \frac{\partial u}{\partial x} = 0, \frac{\partial v}{\partial x} = 0$$

4. RESULTS AND DISCUSSIONS

The characteristics of the flow at the interface of the subsonic diffuser are dominated as listed in Table 1, in order to make comparisons with the results of Dudek et al [6], and Driver and Johnson [14]. A Fortran-90 program has been established to calculate the values of the parameters (ρ , P , T , u , v) from equations that are mentioned previously. The computations have been continued until steady-state solution is satisfied. A CFL factor of 0.01 could be successfully applied to these kinds of problems, as mentioned by Rosello [8]. Usually, about 600-900 iterations are needed to approach the convergence level, and that is better in contrast to thousands of iterations that are mentioned in similar studies.

Table 1 Air properties at the inlet of the diffuser

Property	Value
Density	1.17 kg/m ³
Pressure	100 kPa
Temperature	303 K
Velocity	52 m/s
Viscosity	1.9×10 ⁻⁵ kg/(m.s)
Specific heat	1005 J/(kg.K)
Mach No.	0.15

The variation of the velocity component (u) is presented in the Figures 4, 5 and 6 for many locations in the diffuser (I = 2, I = 12, I = 20). In general, the velocity component (u) decreases along the diffuser, while the velocity component (v) increases. The variation of velocity component (u) in the vertical direction shows decreasing behavior close to the wall (J = 30) due to the effect of viscosity. On the other hand, it shows a constant value at the central points in general (J = 0-20). These results have been compared with those obtained computationally by Dudek et al [6], depending on the code NPARC, as well as the experimental results obtained by Driver and Johnson [14]. The comparison gives similarities at the central points of the diffuser, but quite a few differences (about ±15 %) close to the wall, due to many assumptions considered by their studies, such as, the turbulent flow and the three-dimensional effects.

A high number of grids in the vertical direction are advised in order to seek the velocity drop near the wall due to the boundary layer effect. However, the overall variation of the velocity component (u) inside the diffuser is shown in Figure 7, where it is observed that the decrease in velocity begins in the regions close to the wall and also at the centerline of the inlet, due to the under-relaxation behavior of the computational solution which has settled down rapidly.

Figures 8 and 9 show the variation of pressure and temperature respectively inside the diffuser where both are increasing along the diffuser. It is observed that the increase in the pressure gradient near the wall is more than that in the regions near the centerline, hence, the rapid change. A similar behavior of temperature (as well as density) could be noticed due to the strong relation that collects these parameters.

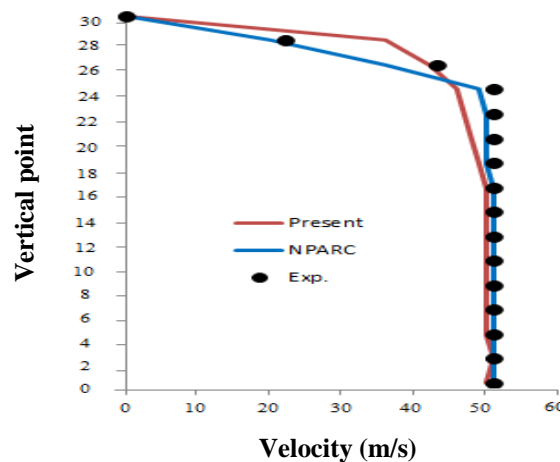


Figure 4 Variation of velocity component (u) at I = 2

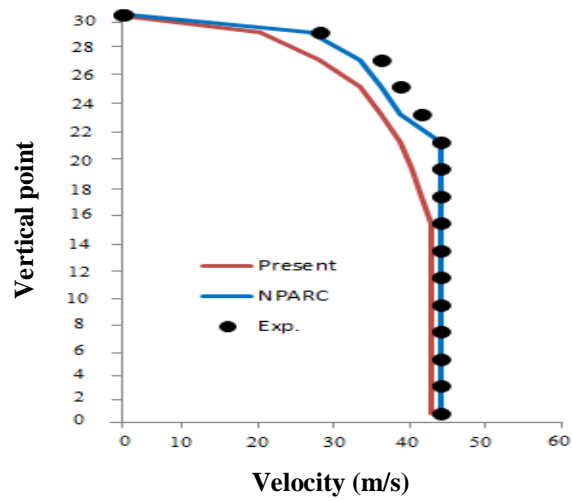


Figure 5 Variation of velocity component (u) at I = 12

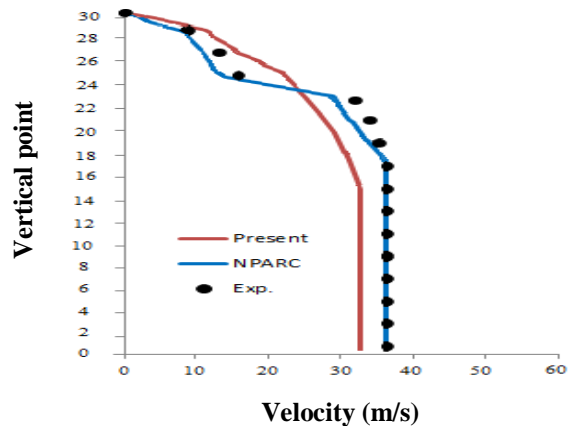


Figure 6 Variation of velocity component (u) at I = 20

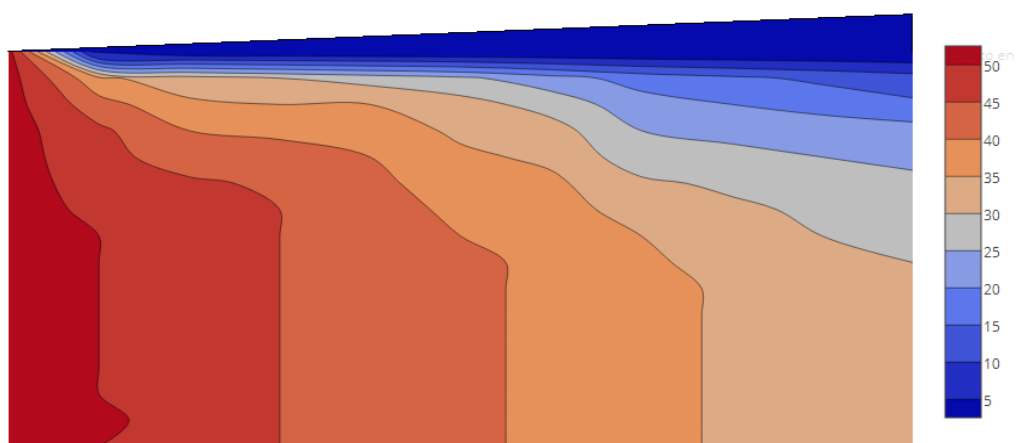


Figure 7 Variation of velocity component (u) in (m/s) inside the diffuser

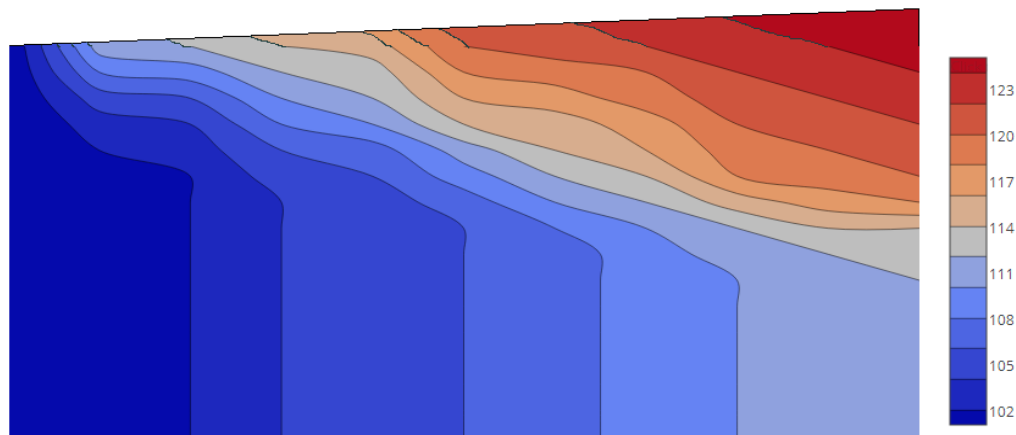


Figure 8 Variation of pressure in (kPa) inside the diffuser

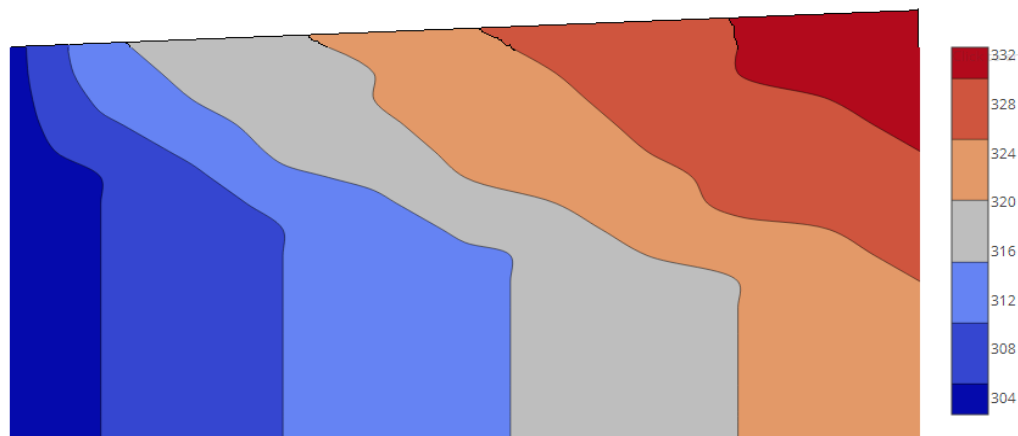


Figure 9 Variation of temperature in (K) inside the diffuser

6. CONCLUSIONS

The direct finite difference method based on the McCormack scheme was used to solve the governing equations of unsteady, viscous (laminar), and compressible flow in a subsonic air diffuser. The following points could be concluded from the current study:

1. The described scheme could be used instead of using ready-made packages such as NPARC or FLUENT, which need to know the adopted codes and expressions.
2. The current numerical method reaches the results faster and more accurately than some numerical mathematical counterparts (such as the Cauchy method). Usually, about 600-900 iterations are needed to approach the convergence level, and that is better in contrast to thousands of iterations that are mentioned by many comparative studies.
3. The grid generation suggested for the diffuser (20 horizontal points times 30 vertical points) was successful. The reason for using a high number of grids in the vertical direction was to catch the velocity drop due to the boundary layer effect near the wall. A CFL factor of 0.01 was suitable.
4. The proposed study can be used to predict the flow in a subsonic air flow inside the diffuser with slight deviation (about $\pm 15\%$) in the values for points close to the wall, compared to the results that were obtained from similar numerical and experimental studies.

References

- [1] Hirsch C., 1997, "Numerical Computation of Internal and External Flows", Vol. 2: "Computational Methods for Inviscid and Viscous Flows", Wiley Series in Numerical Methods in Engineering, John Wiley & Sons
- [2] Abboudi S., Deng J. and Imbert M., 2007, "Thermal Wall Influence on the Behavior of Axisymmetric Laminar Compressible Flow in Nozzle", Journal of Computational and Applied Mechanics, Vol. 8, No. 1, Pages 5–19
- [3] Pardyjak E., "Introduction to Compressible Flow", Notes of Mechanical Engineering Department, University of Utah, www.mech.utah.edu, Accessed on 24/2/2016

- [4] Pauls W., 2010, "On Complex Singularities of the 2D Euler Equation at Short Times", *Physica D* 239, Pages 1159-1169, Elsevier Science Publishing Company
- [5] Swisshelm M., Johnson G. and Kumar S., 1986. "Parallel Computation of Euler and Navier-Stokes Flows, *Applied Mathematics and Computation* Vol. 19, Pages 321-331, Elsevier Science Publishing Company
- [6] Dudek, J.C., N. J. Georgiadis, and D. A. Yoder, 1996, "Calculation of Turbulent Subsonic Diffuser Flows Using the NPARC Navier-Stokes Code", NASA TM, AIAA Paper 96-0497
- [7] Abbood A.H., 1999, "Numerical Analysis of Two-Dimensional Convergent-Divergent Nozzle for A Modern Fighter". MSc. Thesis, College of Military Engineering, Baghdad
- [8] Rosello M., 2002, "Analytic-Numerical Approach to Flow Calculation in Intake and Exhaust Systems of Internal Combustion Engines", *Mathematical and Computer Modelling*, Vol. 36, Pages 33-45
- [9] Jalal M. Jalil and Ahmed F. Kridy, 2009, "Numerical Simulation of a Two-Dimension Ramp Inlet Flow Field", *Engineering and Technology Journal*, Vol. 27, No. 6, Pages 1117-1124
- [10] Sinha P., A.N. Mullick, B. Halder and B. Majumdar, 2011, "Numerical Investigation of Performance Characteristics in Annular Subsonic Diffuser", *IJRMET* Vol. 1, Issue 1, pages 79-83, Oct. 2011
- [11] Berens M., 2015, "Numerical and Experimental Investigations on Subsonic Air Intakes with Serpentine Ducts for UAV Configurations", 5th Air and Space Conference, CEAS, Paper No. 074, 2015
- [12] Anderson D.A., J.C. Tannehill, and R.H. Pletcher, 1984, "Computational Fluid Mechanics and Heat Transfer", McGraw-Hill Company
- [13] Patrick H. Oosthuizen and William E. Carscallen, 1997, "Compressible Fluid Flow", McGraw-Hill Company
- [14] Driver D. M., and Johnson J. P., "Experimental Study of a Three-Dimensional Shear-Driven Turbulent Boundary Layer with Streamwise Adverse Pressure Gradient", NASA TM 102211, May 1990

Nomenclature

E_t	Total energy	J/kg
e	Internal energy	J/kg
P	Pressure	Pa
R	Gas Constant	J/(kg.K)
T	Temperature	K
t	Time	s
u	Horizontal component of the velocity	m/s
v	Vertical component of the velocity	m/s
γ	Specific heat ratio (1.4)	---
μ	Viscosity	kg/(m.s)
ρ	Density	kg/m ³